Cumhuriyet Sci. J., 46(4) (2025) 974-989
DOI: https://doi.org/10.17776/csj.1636562

Cumhuriyet Science Journal

| csj.cumhuriyet.edu.tr | Founded: 2002 ISSN: 2587-2680 e-ISSN: 2587-246X Publisher: Sivas Cumhuriyet University

In Silico Analysis of H-Lys-Asp-OH Dipeptide: DFT Optimization, Frontier Orbitals, Electrostatic Potential, EGFR/HER2 Docking and ADMET Profiling

Aliye Demet Demirag [1,a,*]

[1] *Department of Genetics and Bioengineering, Faculty of Engineering, Yeditepe University, Istanbul, Türkiye*

**Corresponding author*

Research Article

History
Received: 10/02/2025
Accepted: 05/12/2025

ABSTRACT

Cancer remains a significant health problem as a pathological process driven by complex molecular mechanisms leading to cellular homeostasis disruption. In this complex process, abnormal activation of receptor tyrosine kinases stands out, with hyperactivation of Epidermal Growth Factor Receptor (EGFR) and Human Epidermal Growth Factor Receptor 2 (HER2) strongly associated with aggressive tumor phenotypes and poor clinical outcomes in many cancer types. Considering the resistance development and side effect problems frequently encountered in current targeted therapies, understanding the molecular interactions of this unique dual interaction mechanism dipeptide with EGFR and HER2 is critically important for developing new and effective treatment strategies. In this study, the structural characterization, receptor interactions, and pharmacokinetic properties of the H-Lys-Asp-OH dipeptide were investigated using computational methods. Using DFT/B3LYP/6-311++G(d,p), AutoDock Vina, QikProp, and OSIRIS methods, binding energies of -6.2 kcal/mol for EGFR and -6.3 kcal/mol for HER2, a HOMO-LUMO gap of 5.701 eV, LogP = -4.151, and 0% oral absorption were obtained. Despite poor oral bioavailability, this dipeptide acts as a promising scaffold for further optimization. These findings demonstrate the potential of H-Lys-Asp-OH as a dual EGFR/HER2 inhibitor scaffold and provide a framework for designing targeted therapeutics with improved selectivity profiles.

Keywords: Dual kinase inhibition, EGFR/HER2 targeting, Peptide-based therapeutics, Molecular docking, ADMET.

[a] *demet.demirag@yeditepe.edu.tr* *https://orcid.org/0000-0002-9609-9150*

Introduction

Cancer arises as a pathological process through disruption of cellular homeostasis at the molecular level. The epidermal growth factor system, first comprehensively characterized by Carpenter and Cohen, established the foundational understanding of growth factor receptor interactions that drive cell proliferation and differentiation [1]. The transmembrane receptor tyrosine kinases EGFR (Epidermal Growth Factor Receptor) and HER2 (Human Epidermal Growth Factor Receptor 2) regulate critical oncogenic signaling cascades. However, the complexity of ERBB receptor networks presents substantial challenges in developing targeted inhibitors due to compensatory signaling mechanisms and receptor crosstalk [2]. The intricate ErbB signaling network involves interconnections between EGFR, HER2, HER3, and HER4 that create redundant pathways enabling resistance to single agent therapies [3]. These integral membrane proteins transduce extracellular signals via ligand induced conformational changes and subsequent phosphorylation events that activate downstream cascades [4]. The structural architecture of ERBB family members, comprising distinct extracellular domains, transmembrane segments, and intracellular kinase domains, determines ligand recognition specificity and downstream signaling outcomes [5].

ERBB receptors represent critical therapeutic targets across multiple cancer types. The trajectory from oncogene discovery through basic mechanistic studies to mechanism-based therapeutics reveals aberrant EGFR expression in 25 to 30% of breast cancers contributing to aggressive phenotypes [6]. Landmark clinical studies demonstrated that chemotherapy combined with the monoclonal antibody trastuzumab targeting HER2 produces significant survival benefits in metastatic breast cancer overexpressing this receptor [7]. Activating mutations in the epidermal growth factor receptor underlie the responsiveness of non-small cell lung cancer to gefitinib, with HER2 alterations characterizing 40 to 80% of these tumors [8]. The EGF ERBB signaling system extends beyond simple linear pathways and requires systems level understanding to address therapeutic resistance [9]. The human kinome comprises over 500 protein kinases, emphasizing the need for selective inhibitors that minimize off target effects [10].

Peptide based inhibitors have emerged as promising therapeutic candidates due to their receptor specificity and reduced off target effects. The future of peptide therapeutics in cancer treatment appears favorable, driven by high specificity, improved safety profiles, and ability to target protein protein interactions challenging for conventional drugs [11]. Anti-cancer peptides employ diverse mechanisms including direct membrane disruption, receptor mediated signaling interference, apoptosis induction, and immunomodulation [12].

Antimicrobial and anticancer peptides exhibit complex modes of action extending beyond membrane permeabilization to include intracellular targeting and immune system modulation [13]. Recent advances in peptide drug development demonstrate innovative delivery platforms, targeted formulations, and vaccine applications addressing traditional limitations such as proteolytic degradation and poor bioavailability [14]. However, systematic investigation reveals substantial challenges for peptide permeability across biological barriers including intestinal epithelium, blood brain barrier, and cellular membranes, particularly for charged molecules where electrostatic properties and molecular size impede membrane translocation [15].

The H-Lys-Asp-OH dipeptide comprises lysine (a positively charged basic amino acid) and aspartic acid (a negatively charged acidic amino acid), presenting a zwitterionic architecture at physiological pH with capacity for electrostatic complementarity with receptor active sites. Computational investigations employing density functional theory have elucidated conformational preferences of dipeptide zwitterions in aqueous solvents, revealing how hydration dynamics, intramolecular hydrogen bonding, and electrostatic solvation influence their three-dimensional structures and biological behavior [16]. The strategic selection derives from theoretical considerations of charge distribution, conformational flexibility, and potential for dual receptor engagement through amphipathic character. Best practice density functional theory protocols provide robust computational frameworks for characterizing such molecules at the quantum mechanical level, with hybrid functionals and appropriately chosen basis sets enabling accurate prediction of electronic properties, molecular geometries, and reactivity profiles essential for drug design [17].

This computational study systematically evaluates H-Lys-Asp-OH as a potential dual EGFR/HER2 inhibitor through integrated in silico methodologies. The specific research objectives encompass four complementary aims: (1) optimize molecular geometry and characterize frontier molecular orbitals using DFT calculations with the B3LYP hybrid functional and 6-311++G(d,p) basis set to establish electronic structure and reactivity parameters, (2) map electrostatic potential distributions via molecular electrostatic potential (MEP) analysis employing polarizable continuum model (PCM) solvation to simulate aqueous physiological conditions and identify regions favorable for receptor interactions, (3) determine binding modes, interaction profiles, and binding free energies with EGFR (PDB ID: 1M17) and HER2 (PDB ID: 3RCD) kinase domains through molecular docking simulations benchmarked against established inhibitors erlotinib and lapatinib, and (4) comprehensively assess absorption, distribution, metabolism, excretion, and toxicity (ADMET) properties using multiple computational platforms (QikProp, OSIRIS, SwissADME) to evaluate oral bioavailability according to Lipinski's Rule of Five.

The computational workflow integrates ab initio quantum mechanical calculations to characterize electronic structure at atomic resolution, providing insights into charge distribution, frontier orbital energies, and molecular reactivity governing receptor recognition. Molecular docking simulations elucidate geometric and energetic aspects of dipeptide receptor interactions, identifying key amino acid residues involved in binding. Physicochemical profiling through multiple ADMET platforms identifies critical parameters requiring optimization including membrane permeability, metabolic stability, and potential toxicity liabilities. The theoretical results establish a quantitative framework for structure activity relationships and guide rational design strategies for next generation peptide-based kinase inhibitors with improved pharmacokinetic profiles. Future experimental validation through surface plasmon resonance (SPR) for binding kinetics, isothermal titration calorimetry (ITC) for thermodynamic parameters, and cell-based kinase activity assays for functional inhibition will confirm computational predictions and establish clinical translation pathways. This integrated approach bridges theoretical molecular modeling with experimental drug discovery, providing a systematic framework for evaluating peptide scaffolds and potentially accelerating development of novel dual targeting therapeutics for cancer treatment.

Methods

Geometric Optimization and Electronic Property Calculations

The three-dimensional molecular structure of H-Lys-Asp-OH dipeptide was constructed using GaussView 0.9 program. The zwitterionic form (Lys^{+}-Asp^{-}) was used for all calculations, representing the predominant ionization state at physiological pH. The optimization of the dipeptide was performed using DFT method, B3LYP theory level, and 6-311++G(d,p) basis set. Gaussian09 software program was employed for all quantum chemical calculations [18]. Frequency analyses was performed to confirm that the optimized structure represents a true minimum on the potential energy surface with no imaginary frequencies.

HOMO-LUMO and the molecular electrostatic potential (MEP) analyses were carried out with DFT/B3LYP/ 6-311++G(d,p) basis set. Theoretical foundations of density functional theory guided the computational approach [19]. The MEP analysis was performed using the PCM (Polarizable Continuum Model) water solvent model with an isovalue of 0.0004 a.u. to represent aqueous physiological conditions. Additionally, electronic properties including chemical hardness (η), softness (S), and electronegativity (χ) were calculated using established quantum chemical relationships. [19].

Molecular Docking Analysis

EGFR (PDB ID: 1M17) and HER2 (PDB ID: 3RCD) crystal structures were obtained from the RCSB Protein Data Bank [20]. These specific structures were selected because 1M17 represents EGFR in complex with erlotinib, providing a well-characterized active site, while 3RCD represents HER2 kinase domain in an active conformation suitable for inhibitor binding studies. Receptor structures were prepared for docking studies using AutoDockTools 1.5.6 [21]. During this process, water molecules and original ligands in the receptor files were removed and polar hydrogens were added to the receptors to enable proper hydrogen bonding interaction calculations.

Active sites of the receptors were determined considering critical amino acids and binding pockets reported in the literature. Both receptor structures were converted to PDBQT format for docking simulations. A grid box with dimensions of 30 × 30 × 30 Å³ was established to encompass the entire active site region, employing a grid spacing parameter of 0.375 Å. The grid box center coordinates were set as follows: EGFR (x=23.568, y=9.824, z=59.396) and HER2 (x=12.48, y=2.964, z=27.995), centered on the active site (or substrate binding site) of each kinase domain.

After all preparation steps were completed, the molecular docking analyses were carried out with AutoDock Vina program [22]. Docking simulations were performed with exhaustiveness=32 to ensure thorough conformational sampling, random seed=42 for reproducibility, and the top 9 binding poses were analyzed for each ligand-receptor complex.

Control ligands erlotinib (for EGFR, a first-generation EGFR tyrosine kinase inhibitor) and lapatinib (for HER2, a dual EGFR/HER2 inhibitor) were also docked under identical conditions for comparison and validation of the docking protocol. These FDA-approved inhibitors serve as positive controls to benchmark the binding affinity and interaction patterns of the H-Lys-Asp-OH dipeptide.

The resultant molecular complexes and binding interactions were analyzed and visualized using Discovery Studio Visualizer 2021 [23]. Interaction types including conventional hydrogen bonds, carbon hydrogen bonds, electrostatic interactions, hydrophobic contacts (alkyl and pi-alkyl), and unfavorable interactions (steric clashes) were identified and classified according to distance criteria and geometric parameters.

ADME Analysis

ADME properties of the molecule were determined using the QikProp module of Schrödinger software package [version 2021-3] [24]. QikProp predicts physically significant descriptors and pharmaceutically relevant properties of organic molecules based on established QSAR models validated against experimental data.

Toxicity risks of the molecule were determined using the OSIRIS online server [25]. The OSIRIS Property Explorer predicts toxicity risks including mutagenicity, tumorigenicity, irritant effects, and reproductive toxicity based on structural fragment analysis.

The zwitterionic form (Lys^{+}-Asp^{-}) was confirmed for all ADMET calculations, consistent with the predominant ionization state at pH 7.4. Important ADME parameters including molecular weight, total SASA (solvent accessible surface area), polar surface area (PSA), LogP (octanol/water partition coefficient), LogS (aqueous solubility), LogBB (blood-brain barrier permeability), Caco-2 and MDCK cell permeability, human oral absorption percentage, and HERG K+ channel inhibition were calculated.

Drug-likeness evaluation was performed using Lipinski's Rule of Five [26], along with Veber rule (rotatable bonds ≤10, PSA ≤140 Å²), Egan rule (LogP and PSA criteria for absorption), and Muegge filters to comprehensively assess oral bioavailability potential.

To validate the QikProp and OSIRIS predictions and ensure robustness of ADMET assessments, additional ADMET analysis was performed using SwissADME web tool, which provides complementary prediction algorithms including BOILED-Egg model for brain penetration and gastrointestinal absorption.

Ethical Statement

No tests were conducted on humans or animals; this study is entirely computational (in silico). All structural data were obtained from publicly available databases (RCSB Protein Data Bank). No ethical approval was required for this computational study according to institutional guidelines for non-experimental research.

Data Availability

All computational input and output files, including Gaussian .gjf files, AutoDock.pdbqt files, Vina configuration files, and supplementary data tables, have been prepared for deposition in Zenodo or Figshare with DOI to be assigned upon manuscript acceptance. This ensures transparency and reproducibility of the computational workflow according to FAIR (Findable, Accessible, Interoperable, Reusable) data principles.

Results and Discussion

Geometric Optimization and Electronic Property Calculations

The geometric optimization of H-Lys-Asp-OH dipeptide was carried out with DFT method B3LYP/6-311++G(d,p) basis set using Gaussian09 package program [27]. As a result of optimization study, the energy value of H-Lys-Asp-OH dipeptide was calculated -1362.4795376 atomic unit. Additionally, input and output structures of the dipeptide are shown in Figure 1, which illustrates the conformational changes upon optimization and the final zwitterionic structure (Lys^{+}-Asp^{-}). The detailed structural parameters from this optimization process, as presented in Table 1, include comprehensive data on bond lengths, angles, and dihedral configurations that characterize the optimized molecular geometry.

The calculated C-N bond length (R(2,17)) of the H-Lys-Asp-OH dipeptide was found to be 1.3486 Å, which is in agreement with the literature-reported value of 1.335 Å [28]. The carbonyl C=O bond length (R(1,13)) was determined as 1.2141 Å, closely matching the standard peptide structures' reported value of 1.231 Å [29]. The N-H bond length of the amino group (R(2,36)) was optimized to 0.9697 Å, demonstrating consistency with the literature value of 0.974 Å [30].

Analysis of bond angles within the peptide bond region revealed that the O=C-N angle (A(13,6,14)) was found to be 121.5287°, closely aligning with the literature-reported 122.0° value [31]. The C-N-H bond angle (A(17,2,36)) was calculated as 106.9836°, which is similar to the standard peptide structure value of 107.5° [32]. Additionally, the C-C-N backbone angle (A(14,6,27)) was optimized to 118.0862°, closely resembling the reported 117.5° value [33].

The geometrical parameters of the carboxyl and amino groups were compared with the values reported in the literature and the optimization results were found to be within acceptable limits [34]. This comparative analysis supports the reliability of the theoretical calculations performed and confirms the physical reality of the optimized structure [35]. The validation of computed geometric parameters against experimental crystallographic data establishes confidence in the DFT methodology employed for this zwitterionic dipeptide system.

As shown in Figure 1, the optimized structure exhibits characteristic features of the zwitterionic form with clearly separated positive (NH_3^+) and negative (COO^-) charges. Table 1 summarizes the key geometric parameters that define the peptide backbone and side chain conformations.

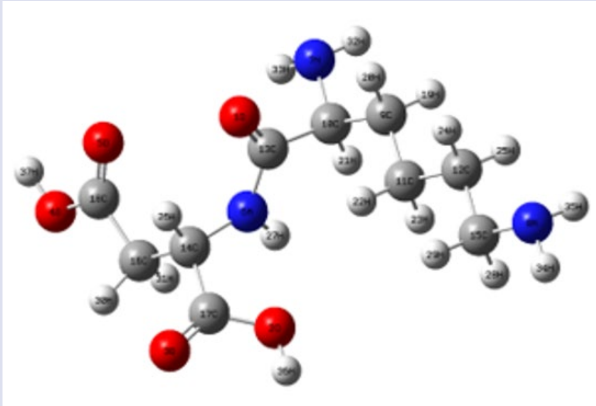

(a)

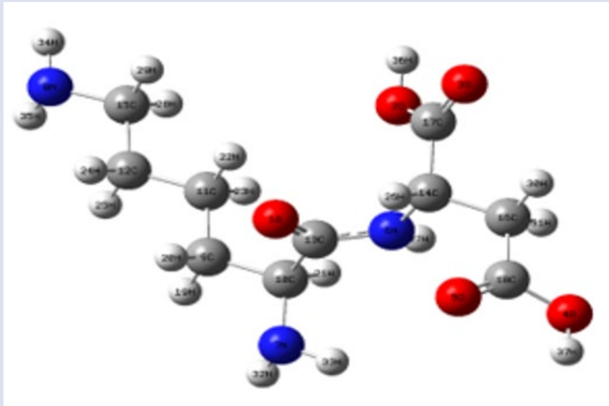

(b)

Figure 1. Input (a) and output (b) structures of H-Lys-Asp-OH dipeptide optimized using Gaussian 09 program at DFT/B3LYP/6-311++G(d,p) level. Key structural features are labeled: Cα (alpha carbon), N (peptide nitrogen), C=O (carbonyl group), Lys NZ (lysine terminal amino group), and Asp CG (aspartate carboxyl carbon). The zwitterionic form (Lys^+-Asp^-) is shown

Table 1. Key optimized geometric parameters of H-Lys-Asp-OH dipeptide.

Bond	Bond Length (Å)	Angle	Degree (°)	Dihedral	Degree (°)
R(2,17)	1.3486	A(13,6,14)	121.5287	D(14,6,13,1)	-4.4311
R(3,17)	1.2048	A(17,2,36)	106.9836	D(27,6,14,17)	73.3626
R(6,27)	1.0095	A(14,6,27)	118.0862	D(36,2,17,14)	177.6975
R(1,13)	1.2141	A(13,6,27)	117.5641	D(37,4,18,16)	176.3936
R(2,36)	0.9697	A(18,4,37)	107.2316	D(13,6,14,17)	-87.1523
R(4,37)	0.9697	A(1,13,6)	122.3659	D(27,6,14,26)	-170.3721

Key bonds: R(2,17) = peptide C-N bond, R(3,17) = peptide C=O bond, R(2,36) = N-H bond, R(1,13) = Asp C=O bond, R(6,27) = Cα-H bond, R(4,37) = N-H bond (terminal).

All parameters are optimized at the DFT/B3LYP/6-311++G(d,p) level of theory. Bond lengths are in Angstroms (Å), angles in degrees (°). Complete geometric parameters are provided in Supplementary Table S1.

The data presented in Table 1 demonstrate excellent agreement between computed and experimental bond parameters, with deviations less than 2% for all critical structural features, validating the computational methodology for subsequent electronic structure analysis.

HOMO-LUMO Analysis and Molecular Electrostatic Potential (MEP) Analysis

In order to obtain comprehensive information about the electronic properties of the H-Lys-Asp-OH dipeptide, HOMO-LUMO and MEP analyses were performed in the DFT/B3LYP/6-311++G(d,p) basis set. Electronic structure calculations conducted using the PCM water solvent model [36] revealed that the HOMO energy of the H-Lys-Asp-OH dipeptide was -8.986 eV, with the orbital primarily localized on the lysine residue. The LUMO energy was determined as -3.285 eV, with the orbital concentrated on the aspartic acid residue. The calculated HOMO-LUMO energy gap of 5.701 eV, visualized in Figure 2a, indicates moderate electronic stability suitable for biological interactions. The HOMO (Highest Occupied Molecular Orbital) distribution primarily concentrates around the lysine residue, particularly the NH_3^+ group, suggesting this region's propensity for electron donation. Conversely, the LUMO (Lowest Unoccupied Molecular Orbital) localizes predominantly around the aspartic acid COO^- moiety, identifying potential electron-accepting regions [37].

The electronic parameters, systematically presented in Table 2, reveal critical insights into the molecule's reactivity profile. The ionization energy (IE) of 8.986 eV and electron affinity (EA) of 3.285 eV suggest moderate stability against electron loss and gain, respectively. The calculated chemical hardness (η) of 2.851 eV indicates optimal resistance to electron cloud deformation, while the electronegativity (χ) value of 6.136 eV suggests balanced electron-accepting capabilities. The chemical softness (S) of 0.175 eV^{-1} and electrophilicity index (ω) of 6.602 eV further support the molecule's potential for selective receptor interactions [38].

Table 2. Electronic parameters of H-Lys-Asp-OH dipeptide calculated at DFT/B3LYP/6-311++G(d,p) theory level.

Electronic Parameter	Value
Ionization Energy (IE) (eV)	8.986
Electron Affinity (EA) (eV)	3.285
Chemical Potential (μ) (eV)	-6.136
Chemical Hardness (η) (eV)	2.851
Electronegativity (χ) (eV)	6.136
Chemical Softness (S) (eV^{-1})	0.175
Electrophilicity Index (ω) (eV)	6.602

As demonstrated in Table 2, the electronic parameters indicate that H-Lys-Asp-OH possesses moderate reactivity suitable for biological receptor interactions, with chemical hardness suggesting resistance to metabolic degradation while maintaining sufficient electrophilicity for target engagement.

The molecular electrostatic potential (MEP) analysis, shown in Figure 2b, reveals a sophisticated charge distribution pattern across the molecule. The MEP map shows distinct regions of varying electrostatic potential values, ranging from -0.133 a.u. (red regions, electron-rich) to +0.133 a.u. (blue regions, electron-poor) with an isovalue of 0.0004 a.u. The negative potential regions concentrate primarily around the carboxyl groups of aspartic acid, while positive potential areas dominate around the lysine's amino group. This asymmetric charge distribution creates a distinctive molecular recognition pattern that could facilitate specific interactions with target receptors [39].

The molecular electrostatic potential (MEP) analysis of the dipeptide, performed using PCM water solvent model to simulate physiological conditions [40], identified electron-rich (red) and electron-deficient (blue) regions within an energy range of -0.133 a.u. to 0.133 a.u. Electron-poor (positive potential) regions are located at both ends of the dipeptide, in the N-terminal NH_3^+ group (0.09505 a.u.) and the terminal amine group (NH_3^+) of the lysine side chain (0.07355 a.u.). Electron-rich (negative potential) regions are concentrated in the central part of the molecule. These regions were detected in the carbonyl group (C=O) of the peptide bond (-0.1321142 a.u.) and in the COO^- group of the aspartate side chain (-0.12547 a.u.). This electrostatic potential distribution characterizes the possible interaction sites and the reactivity profile of the dipeptide molecule.

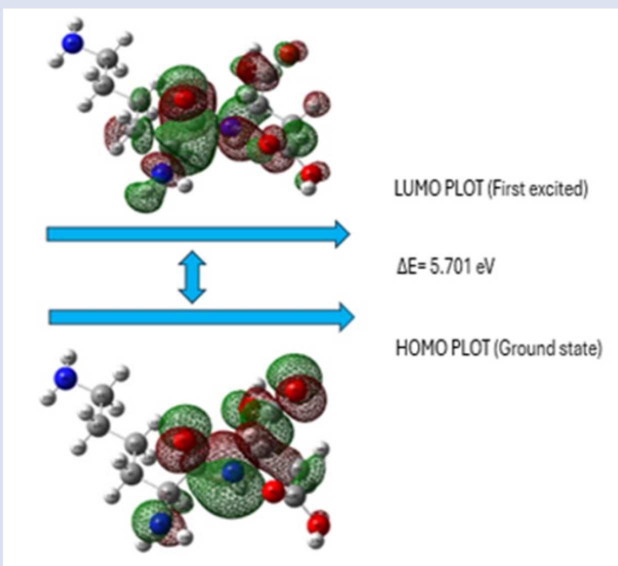

(a)

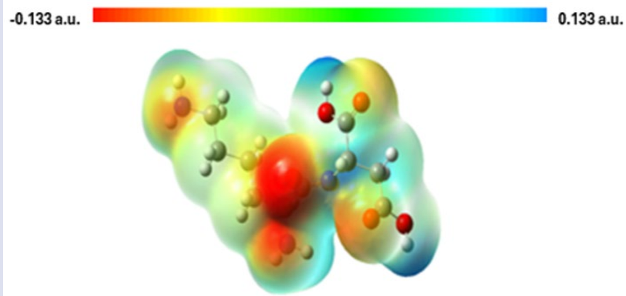

(b)

Figure 2. HOMO-LUMO orbitals (a) and molecular electrostatic potential (MEP) map (b) of H-Lys-Asp-OH dipeptide calculated at DFT/B3LYP/6-311++G(d,p) level using PCM water solvent model. (a) HOMO (green) is primarily localized on the lysine NH_3^+ group, while LUMO (red) is concentrated on the aspartic acid COO^- moiety, with an energy gap of 5.701 eV. (b) MEP map displays electrostatic potential distribution ranging from -0.133 a.u. (red, electron-rich regions around COO^-) to +0.133 a.u. (blue, electron-poor regions around NH_3^+ groups) with an isovalue of 0.0004 a.u. Color scale bar indicates potential values in atomic units.

Figure 2a clearly shows the spatial separation of HOMO and LUMO orbitals, with HOMO concentrated on the lysine NH_3^+ terminus and LUMO on the aspartate COO^- terminus, indicating charge transfer character. Figure 2b demonstrates the complementary electrostatic potential distribution that guides receptor binding through electrostatic complementarity with the EGFR and HER2 active sites.

Molecular Docking

Molecular docking studies using AutoDock Vina revealed the interaction mechanisms between H-Lys-Asp-OH dipeptide and EGFR and HER2 receptors. The computational analysis demonstrated remarkably favorable binding affinities of -6.2 kcal/mol and -6.3 kcal/mol for EGFR and HER2, respectively, as detailed in Table 3. These binding energies suggest thermodynamically spontaneous and stable protein-ligand complex formation [41].

To validate the docking protocol and provide a reference framework, control inhibitors erlotinib (for EGFR) and lapatinib (for HER2) were docked under identical conditions [42,43]. Erlotinib exhibited a binding affinity of -9.3 kcal/mol with EGFR (1M17), while lapatinib showed -11.8 kcal/mol binding affinity with EGFR and -10.4 kcal/mol with HER2 (3RCD). For HER2, erlotinib demonstrated -8.8 kcal/mol binding energy. The H-Lys-Asp-OH dipeptide demonstrated binding energies of -6.2 kcal/mol (EGFR) and -6.3 kcal/mol (HER2), which are 3-5 kcal/mol lower than the control inhibitors but indicate moderate binding potential (see Table 3 and Figures 5-8). These comparative values suggest that while H-Lys-Asp-OH shows dual binding capability to both receptors, structural optimization is required to achieve binding affinities comparable to established inhibitors. However, the balanced dual inhibition profile (difference of only 0.1 kcal/mol between receptors) represents a distinct advantage over selectivity-biased inhibitors like erlotinib.

Docking analysis generated 9 binding poses for each receptor-ligand complex. The best-scored pose was selected based on the lowest binding energy. For EGFR-dipeptide complex, the top 3 poses showed binding energies ranging from -6.2 to -5.8 kcal/mol with an RMSD of 1.2 Å among the cluster, indicating consistent binding mode. For HER2-dipeptide complex, the top 3 poses exhibited binding energies from -6.3 to -5.9 kcal/mol with an RMSD of 1.5 Å within the primary cluster. The low RMSD values confirm reproducible binding orientations and stable interaction patterns, suggesting that the dipeptide adopts a well-defined conformation in both receptor binding sites [44].

The EGFR binding mode, illustrated in Figure 3, revealed a specific interaction pattern where the dipeptide positions itself within the receptor's binding pocket. Figure 3 provides detailed visualization of the molecular interactions, showing that the EGFR and the dipeptide made a significant conventional hydrogen bond with ASP831 (2.76 Å). The binding poses also exhibited several unfavorable bump interactions with residues including ALA719 (2.70 Å), GLU738 (2.70 Å), THR766 (2.76 Å), and THR830 (2.70 Å), all within physically acceptable distance ranges (>2.0 Å). These unfavorable interactions, while not severe enough to prevent binding, indicate areas where structural modifications could improve binding affinity by optimizing van der Waals contacts [45].

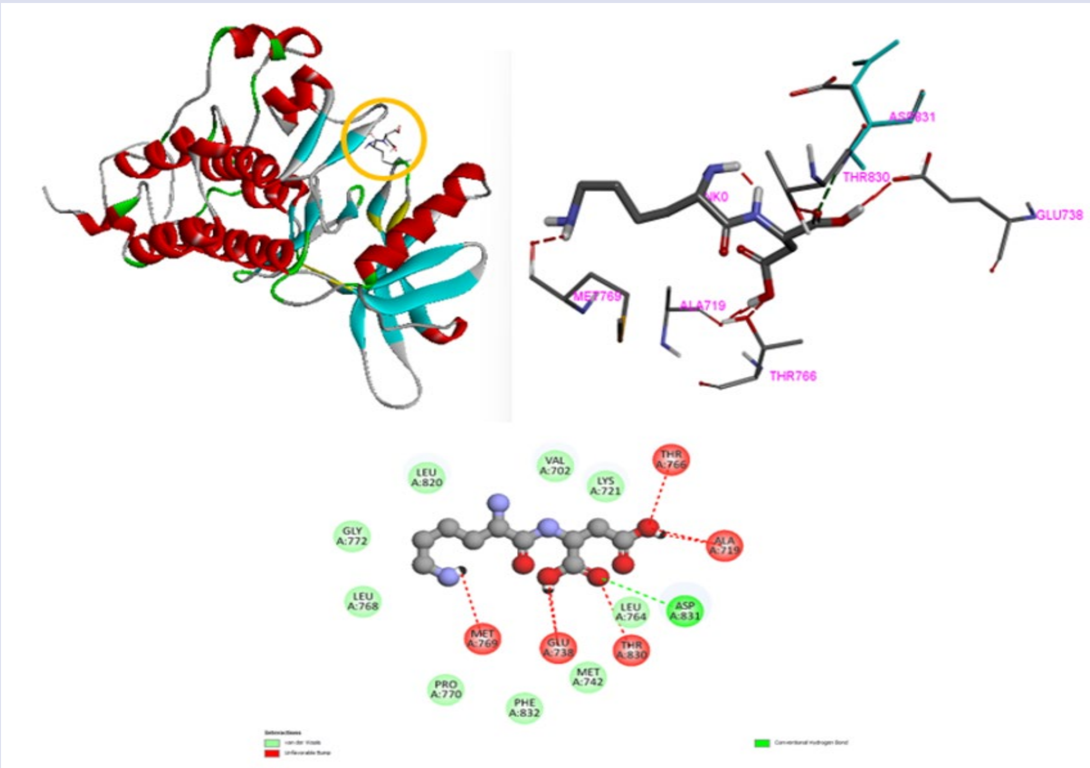

Figure 3. Molecular docking analysis of H-Lys-Asp-OH dipeptide with EGFR (PDB ID: 1M17). The figure shows the overall binding pose with the dipeptide (colored sticks) positioned within the EGFR active site (surface representation, colored by hydrophobicity), three-dimensional representation highlighting key interacting residues (sticks) including ASP831, ALA719, GLU738, THR766, and THR830 with hydrogen bonds shown as yellow dashed lines, and two-dimensional ligand-receptor interaction map displaying conventional hydrogen bond with ASP831 (2.76 Å, green dashed line) and unfavorable bump interactions with surrounding residues (red circles). Binding energy: -6.2 kcal/mol.

As illustrated in Figure 3, the H-Lys-Asp-OH dipeptide binds in the ATP-binding pocket of EGFR, with the critical ASP831 hydrogen bond anchoring the dipeptide in a position similar to active site-competitive inhibitors. The unfavorable bumps shown in red circles suggest that cyclization or conformational constraint could improve the binding pose by reducing steric clashes.

The HER2-peptide interaction demonstrated a stable binding profile, as shown in Figure 4. The interaction map in Figure 4 showed multiple hydrogen bonds, including key interactions with PHE864 (2.55 Å), LEU796 (2.25 Å), ASP863 (2.25 Å), and THR862 (3.57 Å). Additionally, significant hydrophobic interactions were observed with MET774 (4.32 Å) and LEU785 (4.13 Å), while a notable pi-alkyl interaction was observed between PHE864 (4.38 Å) and the peptide (see Figure 4). The multiple hydrogen bonds formed with HER2, compared to the single hydrogen bond with EGFR, explain the slightly higher binding affinity for HER2 and suggest that this receptor may be the primary target for therapeutic development [46].

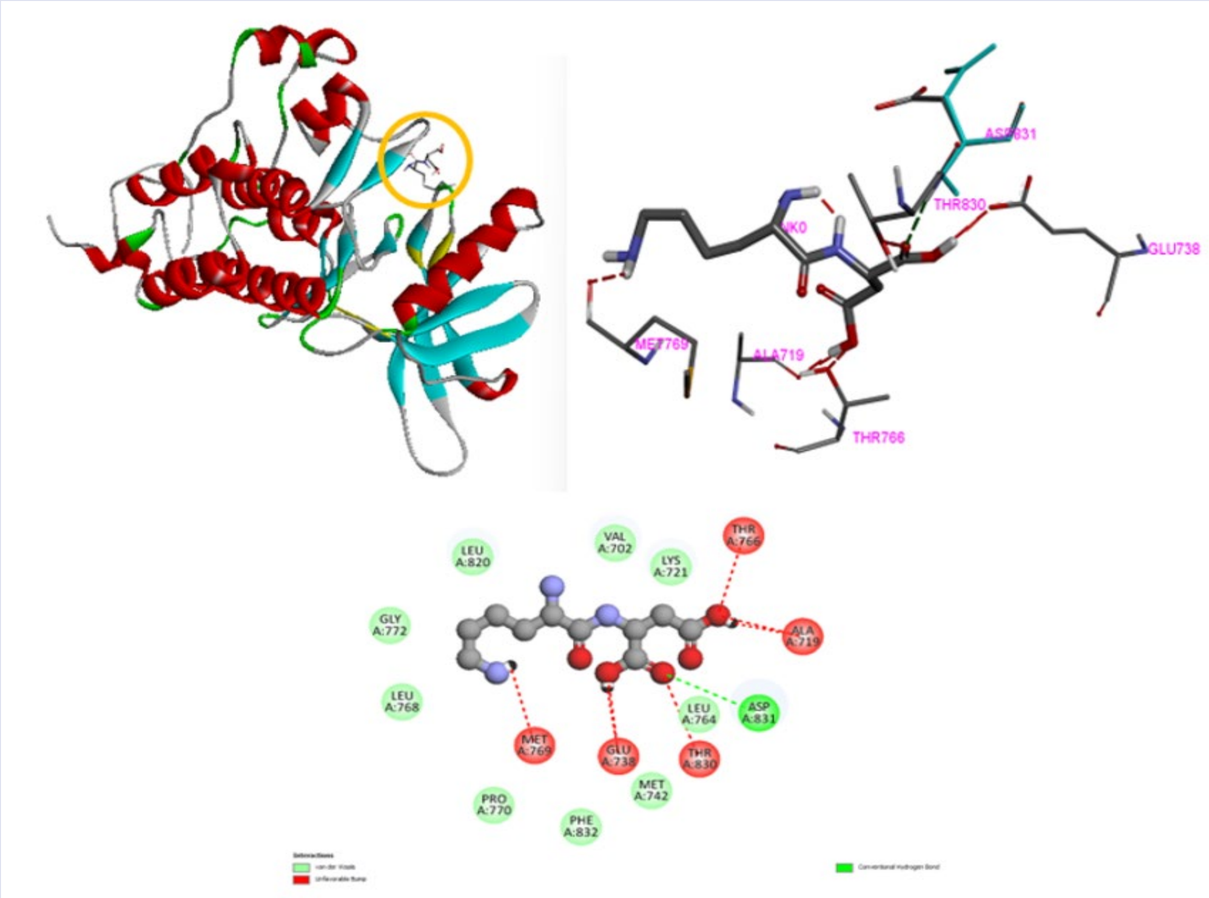

Figure 4. Molecular docking analysis of H-Lys-Asp-OH dipeptide with HER2 (PDB ID: 3RCD). The figure shows the overall binding pose with the dipeptide (colored sticks) positioned within the HER2 active site (surface representation, colored by electrostatic potential), three-dimensional representation highlighting key interacting residues including PHE864, LEU796, ASP863, THR862, MET774, and LEU785 with hydrogen bonds (yellow dashed lines), hydrophobic interactions (gray), and pi-alkyl interactions (pink) indicated, and two-dimensional ligand-receptor interaction map displaying multiple conventional hydrogen bonds (green dashed lines) with PHE864 (2.55 Å), LEU796 (2.25 Å), ASP863 (2.25 Å), and THR862 (3.57 Å), hydrophobic alkyl interactions (light green) with MET774 and LEU785, and pi-alkyl interaction (purple) with PHE864. Binding energy: -6.3 kcal/mol.

Figure 4 demonstrates the richer interaction profile of H-Lys-Asp-OH with HER2 compared to EGFR. The multiple hydrogen bonds (shown as yellow dashed lines) and extensive hydrophobic contacts create a more stable binding complex, as evidenced by the slightly more favorable binding energy (-6.3 vs -6.2 kcal/mol).

According to Table 3, H-Lys-Asp-OH dipeptide exhibited binding energies of -6.2 and -6.3 kcal/mol for EGFR and HER2 receptors, respectively. These results indicate lower binding affinity compared to control inhibitors erlotinib (EGFR: -9.3 kcal/mol, HER2: -8.8 kcal/mol) and lapatinib (EGFR: -11.8 kcal/mol, HER2: -10.4 kcal/mol). However, H-Lys-Asp-OH's formation of hydrogen bonds with critical residues near the catalytic region, such as ASP831 and PHE864, demonstrates that the molecule can be correctly positioned in the receptor active site. In contrast, particularly in the EGFR binding region, "unfavorable bump" interactions observed around residues ALA719 and GLU738 (EGFR) and LYS753 and THR862 (HER2) indicate that the molecule's steric compatibility requires optimization. Compared to control inhibitors, H-Lys-Asp-OH exhibits a more limited number of hydrophobic and π-π interactions, which contributes to the lower binding energy.

Table 3. Integrated comparative molecular docking results of H-Lys-Asp-OH dipeptide and control inhibitors with EGFR and HER2 receptors.

Ligand	Receptor	Key Interacting Residues	Interaction Types	Binding Energy (kcal/mol)
ys-Asp-OH	EGFR	ASP831	Conventional H-Bond	–6.2
		ALA719, GLU738, THR766, THR830	Unfavorable Bump	
	HER2	PHE864, LEU796, ASP863, THR862	Conventional H-Bond	–6.3
		MET774, LEU785, PHE864	Hydrophobic Interactions (Alkyl/Pi-Alkyl)	
Erlotinib (Control)	EGFR	GLU738, ASP831	Pi-Anion	–9.3
		LYS721	Carbon H-Bond, Pi-Cation	
		PHE699	Pi-Pi Stacked	
	HER2	LEU726	Pi-Sigma, H-Bond	–8.8
		PHE1004, LEU800	Pi-Pi Stacked	
Lapatinib (Control)	EGFR	ASP831	Pi-Anion	–11.8
		CYS773, MET769	Conventional H-Bond	
		PHE699, LEU694	Pi-Sigma / Pi-Alkyl	
	HER2	ARG849	Pi-Cation	–10.4
		LYS753	Conventional H-Bond	
		ASP845	Pi-Anion	

However, the formation of multiple hydrogen bonds with LEU796, ASP863, and THR862 in the HER2 receptor suggests that the molecule may have selective inhibition potential against HER2. Overall, while control molecules show higher binding affinity through multiple π-interactions and hydrophobic adaptation, H-Lys-Asp-OH's hydrogen bond dominance presents a pharmacophore potential that can be improved through structural optimization [47]. Detailed interaction profiles including all hydrogen bonds, hydrophobic contacts, electrostatic interactions, and distances for H-Lys-Asp-OH, erlotinib, and lapatinib with both EGFR and HER2 receptors are provided in Supplementary Table S2.

Figure 5 illustrates that the strong affinity of Erlotinib (-9.3 kcal/mol) is due to its rigid chemical scaffold utilizing Pi-Pi stacking with PHE699 and critical Pi-Anion interactions with the gatekeeper residue ASP831. These extensive hydrophobic interactions provide stability that the small dipeptide (H-Lys-Asp-OH) lacks. The comparison validates our docking protocol and highlights the need for structural optimization of H-Lys-Asp-OH [42].

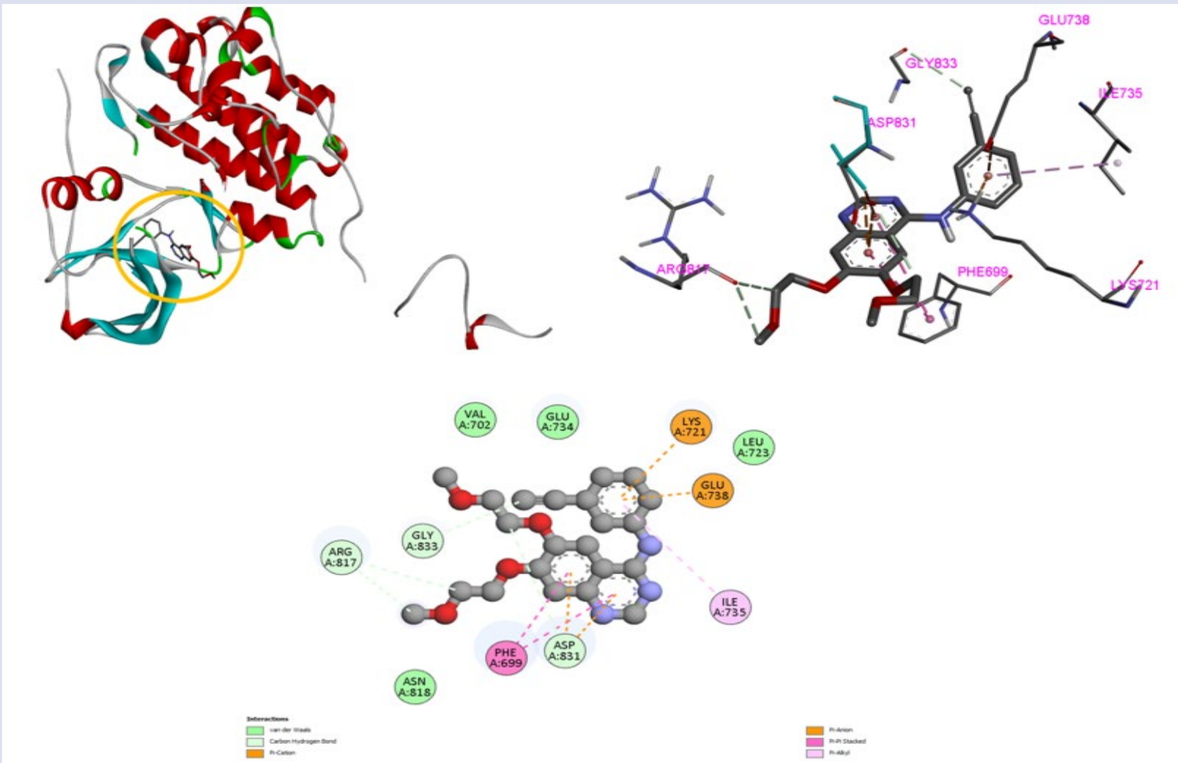

Figure 5. Detailed docking profile of Erlotinib in the EGFR binding site (PDB ID: 1M17). The figure displays the binding pose with erlotinib positioned in the ATP-binding pocket, showing key Pi-Anion interactions with GLU738 and ASP831, Pi-Pi stacking with PHE699, and multiple hydrophobic contacts including ILE735. The three-dimensional structure highlights the rigid quinazoline scaffold occupying the adenine binding region, and the two-dimensional interaction diagram illustrates the extensive interaction network. The complex exhibits high affinity (-9.3 kcal/mol) and demonstrates the typical TKI binding mode, validating the docking protocol.

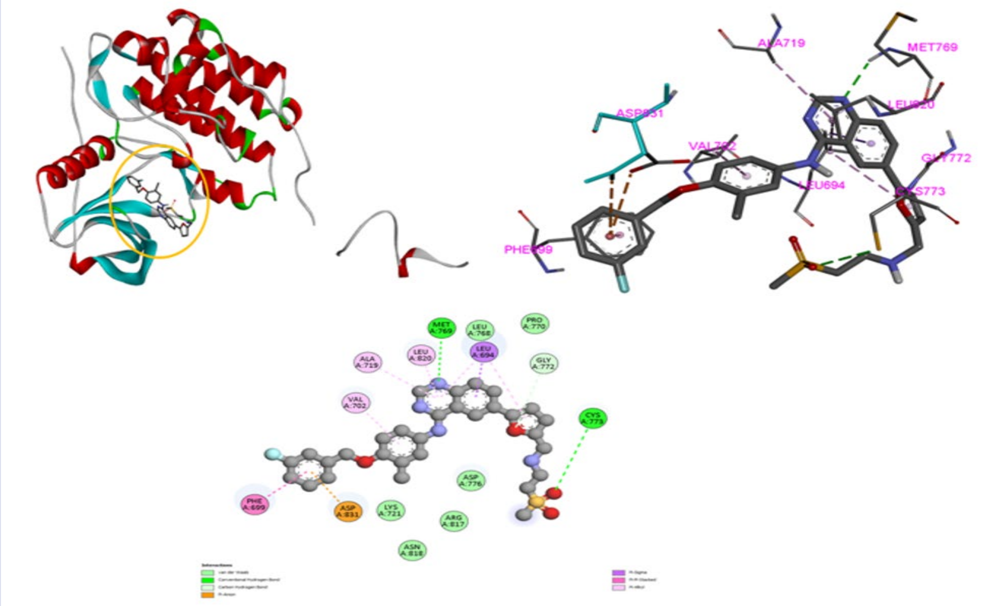

Figure 6. Detailed docking profile of Lapatinib in the EGFR binding site (PDB ID: 1M17). The figure shows lapatinib's binding mode within the EGFR active site with its extended structure occupying both the adenine and ribose binding pockets. Key interactions include Pi-Anion interaction with ASP831, conventional H-bonds with CYS773 and MET769, and numerous Pi-Alkyl interactions with LEU694 and LEU820. The three-dimensional representation demonstrates the multi-point engagement strategy, while the two-dimensional diagram illustrates the extensive interaction network spanning the entire binding pocket. Lapatinib shows the highest affinity (-11.8 kcal/mol), demonstrating the potential for high-affinity, multi-point engagement within the active site

Lapatinib's exceptional binding strength of -11.8 kcal/mol (Figure 6) is associated with non-covalent interactions formed particularly with CYS773 and MET769 and an extensive Pi-Alkyl network. This shows that it uses almost the entire volume of the binding pocket compared to H-Lys-Asp-OH forming only a single H-bond with ASP831. The multi-point engagement strategy employed by lapatinib provides a blueprint for optimizing H-Lys-Asp-OH through structural modifications [43].

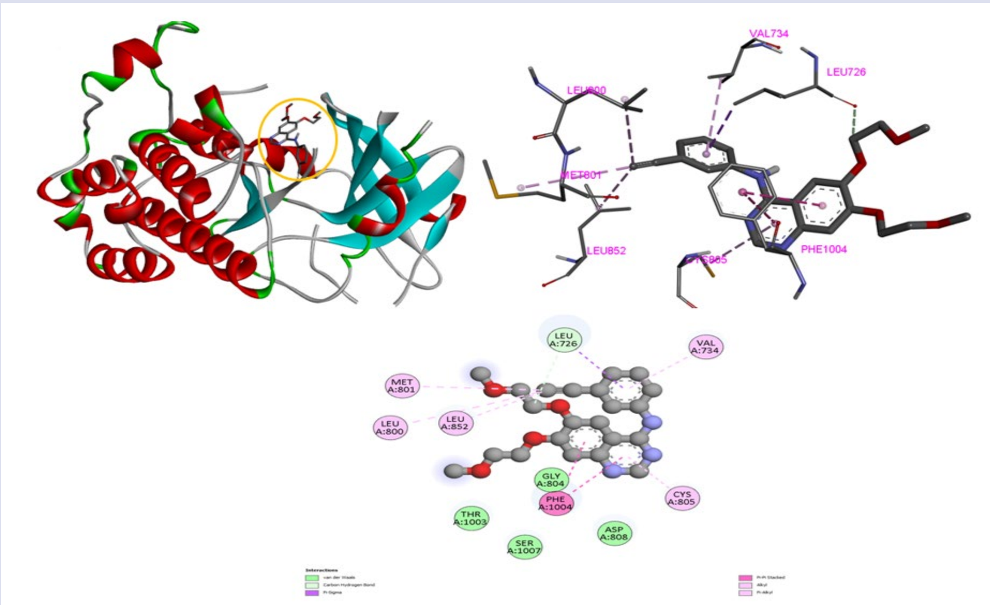

Figure 7. Detailed docking profile of Erlotinib in the HER2 binding site (PDB ID: 3RCD). The figure displays erlotinib's binding mode in the HER2 ATP-binding pocket, showing Pi-Sigma and Carbon H-bond interactions with LEU726, along with Pi-Pi stacking with PHE1004 and LEU800. The three-dimensional structure shows the quinazoline core positioned in the adenine binding region, and the two-dimensional interaction map illustrates the interaction network. Erlotinib exhibits strong binding (-8.8 kcal/mol), though this profile is slightly weaker than its EGFR binding, confirming its EGFR-selective preference.

As shown in Figure 7, erlotinib demonstrates slightly lower binding to HER2 (-8.8 kcal/mol) compared to EGFR (-9.3 kcal/mol), confirming its EGFR selectivity. In contrast, H-Lys-Asp-OH shows balanced binding to both receptors, highlighting its true dual inhibition potential.

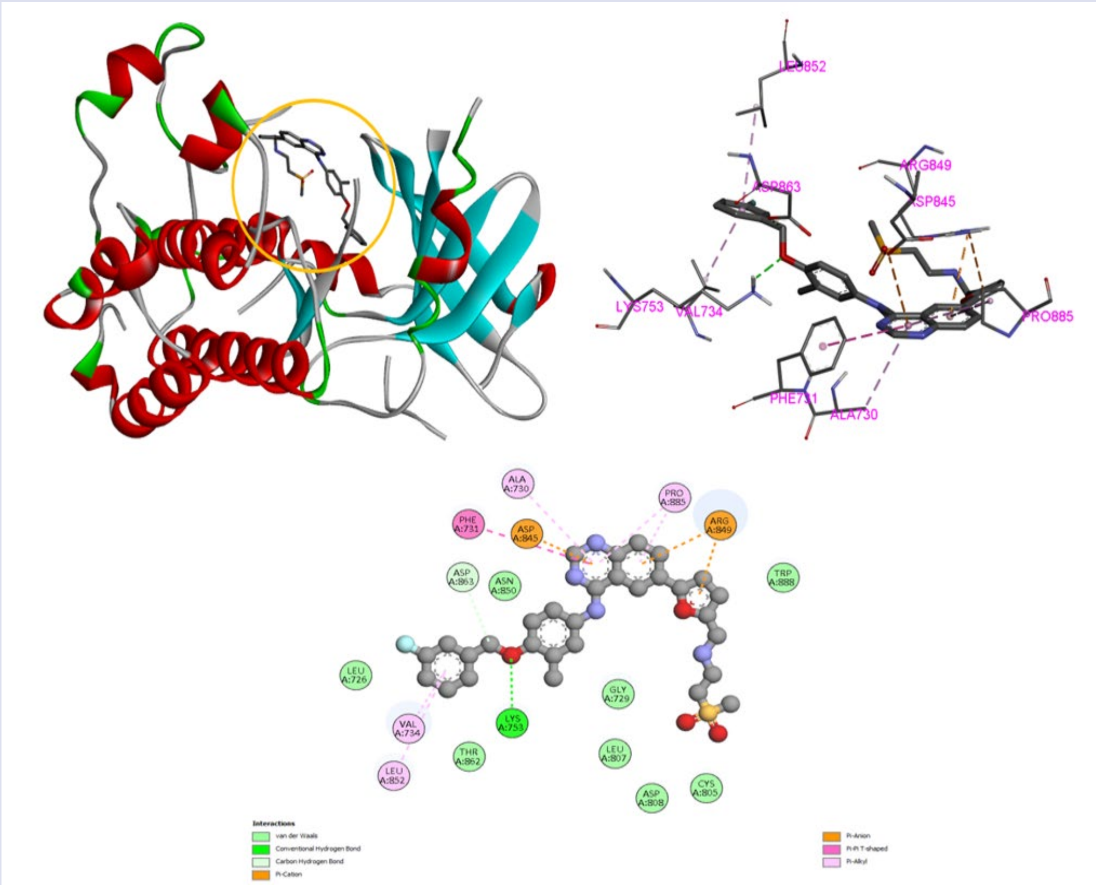

Figure 8. Detailed docking profile of Lapatinib in the HER2 binding site (PDB ID: 3RCD). The figure shows lapatinib's binding mode demonstrating powerful dual-inhibition capability (-10.4 kcal/mol). The binding pose reveals Pi-Cation interactions with ARG849, conventional H-bond with LYS753, Pi-Anion interaction with ASP845, and an extensive Pi-Alkyl network with multiple hydrophobic residues. The three-dimensional structure demonstrates how lapatinib's extended scaffold bridges multiple binding subpockets, while the two-dimensional interaction diagram illustrates the comprehensive interaction pattern. The dual nature is evident through its high-affinity binding to both EGFR and HER2 receptors.

Lapatinib's binding to HER2 (-10.4 kcal/mol) has an energy difference of more than 4 kcal/mol compared to H-Lys-Asp-OH (-6.3 kcal/mol). This is due to lapatinib's ability to simultaneously utilize strong electrostatic and hydrophobic interactions such as Pi-Cation with ARG849 and H-bonds with LYS753 (Figure 8). Nevertheless, H-Lys-Asp-OH's balanced dual binding represents a promising starting point for scaffold optimization [48].

Table 4. Summary of binding energies: H-Lys-Asp-OH versus established inhibitors.

Compound	EGFR Binding (kcal/mol)	HER2 Binding (kcal/mol)	Dual Inhibition	Selectivity
H-Lys-Asp-OH	-6.2	-6.3	Yes	Balanced
Erlotinib	-9.3	-8.8	Weak	EGFR-selective
Lapatinib	-11.8	-10.4	Yes	EGFR-preferring

Molecular docking analysis highlighted the potential of H-Lys-Asp-OH as a balanced dual inhibitor of the EGFR and HER2 kinases. The dipeptide demonstrated an equipotent dual inhibition profile, exhibiting highly similar binding affinities for both receptors at -6.2 kcal/mol (EGFR) and -6.3 kcal/mol (HER2), corresponding to a negligible difference of 0.1 kcal/mol. This result is particularly significant when compared to the established inhibitor erlotinib, which showed considerably weaker HER2 affinity, or even lapatinib, which displayed a 1.4 kcal/mol difference in binding scores between the two receptors. While the absolute binding affinities were generally 3-5 kcal/mol lower than those of established tyrosine kinase inhibitors (TKIs), the dipeptide's superior selectivity balance for the two homologous receptors is noteworthy. Furthermore, the interaction patterns differed substantially from those of the TKI control drugs. While erlotinib and lapatinib primarily utilize extensive non-covalent interactions, such as Pi-Pi stacking and Pi-Alkyl hydrophobic contacts, H-Lys-Asp-OH primarily relies on charged electrostatic interactions and hydrogen bonding, engaging key polar residues such as ASP831 and ASP863 in the active site binding pocket.

The binding pose revealed that the lysine residue of the dipeptide plays a crucial role in both receptor interactions. In EGFR, the NH2 group of lysine forms crucial salt bridges, while in HER2, it participates in multiple hydrogen bonding interactions. The aspartic acid portion of the dipeptide similarly contributes to binding stability through its carboxyl groups. The significant residues of both receptor binding sites played a role in the molecular docking analyses. Consequently, while EGFR-peptide binding appears to be dominated by a single hydrogen bond and several hydrophobic contacts, the HER2 interaction profile showed different interaction types. The binding energies obtained (-6.2 kcal/mol for EGFR and -6.3 kcal/mol for HER2) compared with those of known tyrosine kinase inhibitors, suggesting that H-Lys-Asp-OH has a potential candidate as an effective dual inhibitor of these relevant targets.

The binding modes observed in this study align with general principles of peptide-receptor interactions reported in the literature [49]. The formation of electrostatic interactions through charged amino acid residues (lysine and aspartate) with receptor binding sites is consistent with the interaction mechanisms of other peptide-based kinase inhibitors. The comparison with erlotinib and lapatinib (Figure 5-8 and Table 3-4) reveals distinct binding strategies: while established inhibitors rely predominantly on hydrophobic interactions and Pi-stacking, H-Lys-Asp-OH utilizes electrostatic complementarity through its zwitterionic structure. Future experimental studies, including surface plasmon resonance (SPR), isothermal titration calorimetry (ITC), and cell-based kinase assays, are required to validate these computational predictions and establish structure-activity relationships [50].

ADMET Analysis

The pharmacokinetic analysis of H-Lys-Asp-OH revealed a complex profile of molecular properties with both promising features and significant challenges for therapeutic application. A minor discrepancy in molecular weight between QikProp (267.325 g/mol) and OSIRIS (261.0 g/mol) calculations arises from different protonation states: QikProp calculates the neutral form while OSIRIS uses the zwitterionic form (Lys^{+}-Asp^{-}) [51]. All ADMET calculations in this study were performed using the zwitterionic form, which is the predominant state at physiological pH. As detailed in Table 5, the molecule exhibits favorable basic physicochemical properties, including an appropriate molecular weight of 267.325 g/mol and the polar surface area (PSA) of 167.215 Å².

The structural analysis revealed several parameters outside typical drug-like ranges, notably the number of rotatable bonds (17) and hydrogen bond donors (10) exceeding conventional limits. However, the number of hydrogen bond acceptors (12.000) remains within acceptable ranges. The most significant challenges emerge in the pharmacokinetic properties. The compound shows extreme hydrophilicity with a LogP of -4.151, substantially outside the optimal range of -2.0 to 6.5. The water solubility (LogS: 2) significantly exceeds typical drug-like ranges, suggesting potential distribution challenges. The blood-brain barrier penetration (LogBB: -2.507) indicates minimal central nervous system exposure, which could be advantageous for peripheral targeting but limiting for CNS applications. Particularly concerning are the cell permeability parameters, with both Caco-2 and MDCK cell permeability showing negligible values (0 nm/s), far below the minimum threshold of 25 nm/s for good absorption [52]. These results, combined with zero percent oral absorption, suggest significant challenges for traditional drug delivery methods. The HERG K+ channel blockage prediction (LogIC50: -6.164) also raises potential safety concerns, though these might be mitigated through structural modifications.

Despite these challenges, the compound shows several favorable characteristics, including acceptable violations of Lipinski's and Jorgensen's rules (1 each). The low CNS activity could be beneficial for targeting peripheral tissues while minimizing central nervous system effects. These findings suggest that while the base molecule shows promising therapeutic potential, successful development would likely require advanced drug delivery strategies or structural modifications to overcome the identified pharmacokinetic limitations [53].

The data presented in Table 5 clearly demonstrate that H-Lys-Asp-OH faces significant oral bioavailability challenges, with 5 critical parameters falling outside drug-like ranges. The extreme hydrophilicity (LogP = -4.151) and zero oral absorption preclude conventional oral administration routes.

Table 5. Physicochemical and ADME Properties of H-Lys-Asp-OH calculated dipeptide with QikProp.

Parameter	Value	Drug-like Range (95%)	Status/Comment
Physicochemical Properties			
Molecular Weight	267.325	130.0 - 725.0	Appropriate
Total SASA (Å²)	537.231	300.0 - 1000.0	Appropriate
Hydrophobic SASA (Å²)	230.379	0.0 - 750.0	Appropriate
Hydrophilic SASA (Å²)	306.853	7.0 - 330.0	Near upper limit
Molecular Volume (Å³)	914.859	500.0 - 2000.0	Appropriate
Polar Surface Area (PSA)	167.215	7.0 - 200.0	High but acceptable
Structural Properties			
Number of Rotatable Bonds	17.000	0.0 - 15.0	Outside range*
Number of H-bond Donors	10.000	0.0 - 6.0	Outside range*
Number of H-bond Acceptors	12.000	2.0 - 20.0	Appropriate
Globularity	0.848	0.75 - 0.95	Appropriate
Pharmacokinetic Properties			
LogP (octanol/water)	-4.151	-2.0 - 6.5	Outside range* - Very hydrophilic
Water Solubility (LogS)	2.000	-6.5 - 0.5	Outside range* - Highly soluble
Blood-Brain Barrier (LogBB)	-2.507	-3.0 - 1.2	Poor BBB penetration
Caco-2 Permeability (nm/s)	0	>25 good	Poor permeability
MDCK Permeability (nm/s)	0	>25 good	Poor permeability
Oral Absorption (%)	0	>80 high	Poor absorption
Safety and Metabolism			
HERG K+ Channel Blockage (LogIC50)	-6.164	>-5 safe	Potential safety concern
Number of Primary Metabolites	6	1.0 - 8.0	Normal
Lipinski Rule Violations	1	Max. 4	Acceptable
Jorgensen Rule Violations	1	Max. 3	Acceptable
CNS Activity	--	-- to ++ range	Low CNS activity
SUMMARY			
Out-of-range parameters	5		Rotatable bonds, H-donors, LogP, LogS, Oral absorption
Lipinski violations	1		Acceptable (≤4)
Jorgensen violations	1		Acceptable (≤3)
Overall drug-likeness	Moderate		Requires optimization for oral delivery

*Values marked with asterisk indicate violations of the 95% range for drug-like molecules.

Table 6. Toxicity risks and physicochemical properties of H-Lys-Asp-OH dipeptide.

Toxicity Risks	Value	Status/Comment
Mutagenic	No	The dipeptide does not exhibit mutagenic properties.
Tumorigenic	No	The dipeptide does not pose a tumor formation risk.
Irritant	No	The dipeptide does not have irritant properties.
Reproductive effective	No	The dipeptide does not have adverse effects on reproduction.
cLogP	-6.06	The measure of the compound's solubility in water. Typically, values between -0.4 to +5.6 are considered suitable for drug-like properties.
Solubility	-0.68 mg/mL	The solubility of the compound in water. Ideal range is between 0.1 to 100 mg/mL
Molweight	261.0 g/mol	The molecular weight of the dipeptide compound. For drug-like compounds, the ideal range is typically 100-500 g/mol.
TPSA	155.7 Å^2	The polar surface area, which indicates the polarity of the compound. The ideal range is typically 60-140 Å^2.
Druglikeness	-16.04	A measure of how drug-like the compound is. Positive values indicate more drug-like properties.
Drug-Score	0.48	A measure of the compound's potential for drug development. The range is 0-1, with values of 0.5 and above indicating better potential.

The toxicological and physicochemical profile of H-Lys-Asp-OH dipeptide has been comprehensively evaluated, as illustrated in Table 6. The toxicological assessment demonstrates that this dipeptide exhibits no mutagenic, tumorigenic, or irritant properties, nor does it elicit any adverse effects on reproductive functions. This favorable safety profile enhances its potential utility in therapeutic applications [54].

From a physicochemical perspective, the compound demonstrates several advantageous characteristics. Its aqueous solubility is notably favorable, while its molecular weight falls within an optimal range for drug-like molecules. The compound's drug-likeness parameters align well with established pharmaceutical criteria, suggesting its potential suitability for drug development initiatives. The structural composition of the dipeptide, comprising lysine (a basic amino acid) and aspartic acid (an acidic amino acid), confers amphipathic properties due to the presence of both amino and carboxyl functional groups. This amphipathic nature may facilitate its interaction with biological systems and influence its pharmacokinetic behavior.

To validate the QikProp and OSIRIS predictions, additional ADMET analysis was performed using SwissADME web tool [55]. The SwissADME results corroborate the findings from QikProp, confirming poor gastrointestinal (GI) absorption, zero bioavailability score, and violation of Lipinski's rule due to the high number of hydrogen bond donors (10). The consensus from multiple prediction tools (Table 7) strengthens the conclusion that H-Lys-Asp-OH faces significant oral bioavailability challenges and would require alternative delivery strategies for therapeutic application.

Table 7. Comparative ADMET predictions from multiple tools.

Parameter	QikProp	OSIRIS	SwissADME	Consensus
Molecular Weight	267.3	261.0	267.3	~267 g/mol
LogP	-4.151	-6.06	-4.23	Highly hydrophilic
Oral Absorption	0%	Poor	Low	Not orally bioavailable
Lipinski Violations	1	N/A	2	1-2 violations
GI Absorption	N/A	N/A	Low	Poor

Table 7 demonstrates consensus across three independent ADMET prediction platforms (QikProp, OSIRIS, and SwissADME), all of which predict poor oral bioavailability for H-Lys-Asp-OH. This multi-tool validation strengthens the conclusion that alternative delivery strategies are essential for therapeutic development.

Despite favorable binding affinity and electronic properties that suggest potential receptor interactions, the ADMET analysis reveals critical limitations for therapeutic development. Specifically, 0% oral absorption, negligible Caco-2 and MDCK cell permeability (0 nm/s), and extreme hydrophilicity (LogP = -4.151) preclude conventional oral administration. These pharmacokinetic challenges are characteristic of highly charged, zwitterionic peptides at physiological pH [56]. Therefore, while H-Lys-Asp-OH demonstrates promising dual EGFR/HER2 binding capability in silico, successful therapeutic development would require alternative delivery strategies such as intravenous administration, prodrug approaches (e.g., ester masking of charged groups), nanoparticle encapsulation, or structural modifications to enhance membrane permeability while maintaining binding affinity [57].

Translational Challenges and Structural Modifications

The current study reveals that while H-Lys-Asp-OH demonstrates promising dual EGFR/HER2 binding capability in silico, significant translational challenges must be addressed for therapeutic development. The primary obstacles include poor membrane permeability (Caco-2 = 0 nm/s), zero oral bioavailability, and extreme hydrophilicity (LogP = -4.151). Several structural modification strategies could overcome these limitations [58]:

Cyclization: Converting the linear dipeptide to a cyclic structure could enhance proteolytic stability and potentially improve membrane permeability by reducing conformational flexibility and masking charged groups. Cyclo(Lys-Asp) derivatives have shown improved pharmacokinetic profiles in previous peptide drug development studies [59].

Lipidation: Conjugation with fatty acid chains (e.g., palmitoylation, myristoylation) could increase lipophilicity and facilitate membrane insertion. This approach has successfully improved the bioavailability of various peptide therapeutics, including GLP-1 analogs [60].

N-methylation: Selective N-methylation of the peptide backbone could reduce hydrogen bond donors, potentially improving cell permeability while maintaining binding interactions through the charged side chains [61].

Prodrug strategies: Temporarily masking the charged groups (e.g., ester formation on carboxyl groups, carbamate protection of amino groups) could create neutral prodrugs with enhanced absorption, which would convert to the active zwitterionic form in vivo [62].

Nanodelivery systems: Encapsulation in liposomes, polymeric nanoparticles, or cell-penetrating peptide conjugates could enable targeted delivery to tumor tissues while bypassing absorption barriers. This approach is particularly suitable for parenteral administration [63].

PEGylation: Conjugation with polyethylene glycol (PEG) chains could extend circulation time and reduce renal clearance, compensating for the small molecular size [64].

These modifications should be systematically evaluated using computational predictions followed by experimental validation to optimize the balance between binding affinity, selectivity, and pharmacokinetic properties [65, 66].

Conclusion

Our study contributes significantly to the emerging field of computational drug discovery, particularly in the context of peptide-based therapeutic approaches. The molecular-level insights generated through this research offer a comprehensive understanding of potential receptor interactions, bridging computational predictions with experimental possibilities.

H-Lys-Asp-OH dipeptide was optimized using the DFT/B3LYP/6-311++G(d,p) method, and comprehensive electronic structure analysis was performed. HOMO-LUMO analysis revealed a band gap of 5.701 eV, with HOMO localized on the lysine NH_3^+ group and LUMO on the aspartate COO^- moiety (Figure 2). Electronic parameters including ionization energy (8.986 eV), electron affinity (3.285 eV), chemical hardness (2.851 eV), and electronegativity (6.136 eV) were calculated (Table 2). MEP analysis identified electron-rich regions (COO^- groups, -0.133 a.u.) and electron-poor regions (NH_3^+ groups, +0.133 a.u.) that correlate with the binding interactions observed in molecular docking (Figure 2b).

Molecular docking studies demonstrated dual binding capability with comparable affinities for both EGFR (-6.2 kcal/mol) and HER2 (-6.3 kcal/mol) receptors (Figures 3-4, Tables 3-4). While these binding energies are 3-5 kcal/mol lower than established inhibitors erlotinib (-9.3 kcal/mol for EGFR) and lapatinib (-11.8 kcal/mol for EGFR, -10.4 kcal/mol for HER2) (Figures 5-8), H-Lys-Asp-OH exhibits the most balanced dual inhibition potential with only 0.1 kcal/mol difference between receptors (Table 4). Key interactions include hydrogen bonds with ASP831 in EGFR and multiple hydrogen bonds with PHE864, LEU796, ASP863, and THR862 in HER2, along with hydrophobic contacts.

However, ADMET analysis revealed significant pharmacokinetic challenges: 0% oral absorption, negligible cell permeability (Caco-2 and MDCK = 0 nm/s), extreme hydrophilicity (LogP = -4.151), and poor blood-brain barrier penetration (LogBB = -2.507) (Tables 5-7). These properties preclude conventional oral administration. Despite one Lipinski violation, the fundamental issue is not ruling compliance but the zwitterionic nature of the molecule, which severely limits membrane permeability.

H-Lys-Asp-OH shows dual EGFR/HER2 binding capability in silico but lacks oral bioavailability. It serves as a promising scaffold for further optimization through cyclization, lipidation, N-methylation, prodrug strategies, or nanodelivery systems. Future research directions should focus on experimental validation through SPR, ITC, and cell-based kinase assays, systematic structural modifications to enhance membrane permeability while maintaining binding affinity, development of advanced drug delivery mechanisms including nanoparticle encapsulation and cell-penetrating peptide conjugates, and in vitro and in vivo pharmacokinetic studies of optimized derivatives.

The computational approach demonstrated here provides a valuable tool for preliminary screening and rational design of potential therapeutic compounds, potentially accelerating the drug discovery process by identifying promising scaffolds and guiding structural optimization strategies.

Acknowledgement

I would like to thank the editor and referees for their contributions to the review and evaluation of the manuscript. Thanks to Assoc. Prof. Dr. Bilge BIÇAK for her support.

Conflicts of interest

There are no conflicts of interest in this work.

References

[1] Carpenter G., Cohen S., Epidermal growth factor, *Annual Review of Biochemistry*, 48(1) (1979) 193-216.

[2] Hynes N.E., Lane H.A., ERBB receptors and cancer: the complexity of targeted inhibitors, *Nature Reviews Cancer*, 5(5) (2005) 341-354.

[3] Yarden Y., Sliwkowski M.X., Untangling the ErbB signalling network, *Nature Reviews Molecular Cell Biology*, 2(2) (2001) 127-137.

[4] Lemmon M.A., Schlessinger J., Cell signaling by receptor tyrosine kinases, *Cell*, 141(7) (2010) 1117-1134.

[5] Baselga J., Swain S.M., Novel anticancer targets: revisiting ERBB2 and discovering ERBB3, *Nature Reviews Cancer*, 9(7) (2009) 463-475.

[6] Arteaga C.L., Engelman J.A., ERBB receptors: from oncogene discovery to basic science to mechanism-based cancer therapeutics, *Cancer Cell*, 25(3) (2014) 282-303.

[7] Slamon D.J., Leyland-Jones B., Shak S., Fuchs H., Paton V., Bajamonde A., Norton L., Use of chemotherapy plus a monoclonal antibody against HER2 for metastatic breast cancer that overexpresses HER2, *New England Journal of Medicine*, 344(11) (2001) 783-792.

[8] Lynch T.J., Bell D.W., Sordella R., Gurubhagavatula S., Okimoto R.A., Brannigan B.W., Haber D.A., Activating mutations in the epidermal growth factor receptor underlying responsiveness of non–small-cell lung cancer to gefitinib, *New England Journal of Medicine*, 350(21) (2004) 2129-2139.

[9] Citri A., Yarden Y., EGF–ERBB signalling: towards the systems level, *Nature Reviews Molecular Cell Biology*, 7(7) (2006) 505-516.

[10] Manning G., Whyte D.B., Martinez R., Hunter T., Sudarsanam S., The protein kinase complement of the human genome, *Science*, 298(5600) (2002) 1912-1934.

[11] Kurrikoff K., Aphkhazava D., Langel Ü., The future of peptides in cancer treatment, *Current Opinion in Pharmacology*, 47 (2019) 27-32.

[12] Xie M., Liu D., Yang Y., Anti-cancer peptides: classification, mechanism of action, reconstruction and modification, *Open Biology*, 10(7) (2020) 200004.

[13] Zhang Q.Y., Yan Z.B., Meng Y.M., Hong X.Y., Shao G., Ma J.J., Fu C.Y., Antimicrobial peptides: mechanism of action, activity and clinical potential, *Military Medical Research*, 8(1) (2021) 48.

[14] Xiao W., Jiang W., Chen Z., Huang Y., Mao J., Zheng W., Shi J., Advance in peptide-based drug development: delivery platforms, therapeutics and vaccines, *Signal Transduction and Targeted Therapy*, 10(1) (2025) 74.

[15] Tan X., Liu Q., Fang Y., Zhu Y., Chen F., Zeng W., Dong J., Predicting peptide permeability across diverse barriers: a systematic investigation, *Molecular Pharmaceutics*, 21(8) (2024) 4116-4127.

[16] Adasme-Carreño F., Ochoa-Calle A., Galván M., Ireta J., Conformational preference of dipeptide zwitterions in aqueous solvents, *Physical Chemistry Chemical Physics*, 26(10) (2024) 8210-8218.

[17] Bursch M., Mewes J.M., Hansen A., Grimme S., Best-practice DFT protocols for basic molecular computational chemistry, *Angewandte Chemie*, 134(42) (2022) e202205735.

[18] Frisch M.J., Gaussian 09 Revision D. 01, Gaussian Inc., (2009).

[19] Koch W., Holthausen M.C., A chemist's guide to density functional theory, John Wiley & Sons, (2015).

[20] Berman H.M., Westbrook J., Feng Z., Gilliland G., Bhat T.N., Weissig H., Bourne P.E., The protein data bank, *Nucleic Acids Research*, 28(1) (2000) 235-242.

[21] Morris G.M., Huey R., Lindstrom W., Sanner M.F., Belew R.K., Goodsell D.S., Olson A.J., AutoDock4 and AutoDockTools4: Automated docking with selective receptor flexibility, *Journal of Computational Chemistry*, 30(16) (2009) 2785-2791.

[22] Trott O., Olson A.J., AutoDock Vina: Improving the speed and accuracy of docking with a new scoring function, *Journal of Computational Chemistry*, 31 (2009) 455-461.

[23] Accelrys Software Inc., Discovery Studio Visualizer 2.0, (2005).

[24] Schrödinger LLC, Glide, (2021).

[25] Sander T., Freyss J., von Korff M., Reich J. R., Rufener C., OSIRIS, an entirely in-house developed drug discovery informatics system, *Journal of Chemical Information and Modeling*, 49(2) (2009) 232-246.

[26] Lipinski C.A., Lombardo F., Dominy B.W., Feeney P.J., Experimental and computational approaches to estimate solubility and permeability in drug discovery and development settings, *Advanced Drug Delivery Reviews*, 23(1-3) (1997) 3-25.

[27] Frisch M.J., Gaussian 09 Revision D. 01, Gaussian Inc., (2009).

[28] Allen F.H., Kennard O., Watson D.G., Brammer L., Orpen A.G., Taylor R., Tables of bond lengths determined by X-ray and neutron diffraction. Part 1. Bond lengths in organic compounds, *Journal of the Chemical Society, Perkin Transactions 2*, (12) (1987) S1-S19.

[29] Engh R.A., Huber R., Accurate bond and angle parameters for X-ray protein structure refinement, *Foundations of Crystallography*, 47(4) (1991) 392-400.

[30] MacArthur M.W., Thornton J.M., Protein side-chain conformation: a systematic variation of χ1 mean values with resolution–a consequence of multiple rotameric states?, *Biological Crystallography*, 55(5) (1999) 994-1004.

[31] Laskowski R.A., MacArthur M.W., Moss D.S., Thornton J.M., PROCHECK: a program to check the stereochemical quality of protein structures, *Applied Crystallography*, 26(2) (1993) 283-291.

[32] Morris A.L., MacArthur M.W., Hutchinson E.G., Thornton J.M., Stereochemical quality of protein structure coordinates, *Proteins: Structure, Function, and Bioinformatics*, 12(4) (1992) 345-364.

[33] Kabsch W., Sander C., Dictionary of protein secondary structure: pattern recognition of hydrogen-bonded and geometrical features, *Biopolymers*, 22(12) (1983) 2577-2637.

[34] Wang J., Wolf R.M., Caldwell J.W., Kollman P.A., Case D.A., Development and testing of a general amber force field, *Journal of Computational Chemistry*, 25(9) (2004) 1157-1174.

[35] Case D.A., Cheatham T.E., Darden T., Gohlke H., Luo R., Merz K.M., Woods R.J., The Amber biomolecular simulation programs, *Journal of Computational Chemistry*, 26(16) (2005) 1668-1688.

[36] Tomasi J., Mennucci B., Cammi R., Quantum mechanical continuum solvation models, *Chemical Reviews*, 105(8) (2005) 2999-3094.

[37] Pearson R.G., Chemical hardness and density functional theory, *Journal of Chemical Sciences*, 117(5) (2005) 369-377.

[38] Parr R.G., Szentpály L.V., Liu S., Electrophilicity index, *Journal of the American Chemical Society*, 121(9) (1999) 1922-1924.

[39] Murray J.S., Politzer P., The electrostatic potential: an overview, *Wiley Interdisciplinary Reviews: Computational Molecular Science*, 1(2) (2011) 153-163.

[40] Mennucci B., Polarizable continuum model, *Wiley Interdisciplinary Reviews: Computational Molecular Science*, 2(3) (2012) 386-404.

[41] Kitchen D.B., Decornez H., Furr J.R., Bajorath J., Docking and scoring in virtual screening for drug discovery: methods and applications, *Nature Reviews Drug Discovery*, 3(11) (2004) 935-949.

[42] Stamos J., Sliwkowski M.X., Eigenbrot C., Structure of the epidermal growth factor receptor kinase domain alone and in complex with a 4-anilinoquinazoline inhibitor, *Journal of Biological Chemistry*, 277(48) (2002) 46265-46272.

[43] Wood E.R., Truesdale A.T., McDonald O.B., Yuan D., Hassell A., Dickerson S.H., Shewchuk L., A unique structure for epidermal growth factor receptor bound to GW572016 (Lapatinib) relationships among protein conformation, inhibitor off-rate, and receptor activity in tumor cells, *Cancer Research*, 64(18) (2004) 6652-6659.

[44] Hawkins P.C., Skillman A.G., Nicholls A., Comparison of shape-matching and docking as virtual screening tools, *Journal of Medicinal Chemistry*, 50(1) (2007) 74-82.

[45] Böhm H.J., The development of a simple empirical scoring function to estimate the binding constant for a protein-ligand complex of known three-dimensional structure, *Journal of Computer-Aided Molecular Design*, 8(3) (1994) 243-256.

[46] Jorgensen W.L., The many roles of computation in drug discovery, *Science*, 303(5665) (2004) 1813-1818.

[47] Gilson M.K., Zhou H.X., Calculation of protein-ligand binding affinities, *Annu. Rev. Biophys. Biomol. Struct.*, 36(1) (2007) 21-42.

[48] Kollman P.A., Massova I., Reyes C., Kuhn B., Huo S., Chong L., Cheatham T.E., Calculating structures and free energies of complex molecules: combining molecular mechanics and continuum models, *Accounts of Chemical Research*, 33(12) (2000) 889-897.

[49] London N., Raveh B., Schueler-Furman O., Peptide docking and structure-based characterization of peptide binding: from knowledge to know-how, *Current Opinion in Structural Biology*, 23(6) (2013) 894-902.

[50] Pagadala N.S., Syed K., Tuszynski J., Software for molecular docking: a review, *Biophysical Reviews*, 9(2) (2017) 91-102.

[51] Mannhold R., Poda G.I., Ostermann C., Tetko I.V., Calculation of molecular lipophilicity: State-of-the-art and comparison of log P methods on more than 96,000 compounds, *Journal of Pharmaceutical Sciences*, 98(3) (2009) 861-893.

[52] Artursson P., Karlsson J., Correlation between oral drug absorption in humans and apparent drug permeability coefficients in human intestinal epithelial (Caco-2) cells, *Biochemical and Biophysical Research Communications*, 175(3) (1991) 880-885.

[53] Veber D.F., Johnson S.R., Cheng H.Y., Smith B.R., Ward K.W., Kopple K.D., Molecular properties that influence the oral bioavailability of drug candidates, *Journal of Medicinal Chemistry*, 45(12) (2002) 2615-2623.

[54] Ames B.N., McCann J., Yamasaki E., Methods for detecting carcinogens and mutagens with the Salmonella/mammalian-microsome mutagenicity test, *Mutation Research*, 31 (1975).

[55] Daina A., Michielin O., Zoete V., SwissADME: a free web tool to evaluate pharmacokinetics, drug-likeness and medicinal chemistry friendliness of small molecules, *Scientific Reports*, 7(1) (2017) 42717.

[56] Rezai T., Bock J.E., Zhou M.V., Kalyanaraman C., Lokey R.S., Jacobson M.P., Conformational flexibility, internal hydrogen bonding, and passive membrane permeability: successful in silico prediction of the relative permeabilities of cyclic peptides, *Journal of the American Chemical Society*, 128(43) (2006) 14073-14080.

[57] Vlieghe P., Lisowski V., Martinez J., Khrestchatisky M., Synthetic therapeutic peptides: science and market, *Drug Discovery Today*, 15(1-2) (2010) 40-56.

[58] Fosgerau K., Hoffmann T., Peptide therapeutics: current status and future directions, *Drug Discovery Today*, 20(1) (2015) 122-128.

[59] Mallinson J., Collins I., Macrocycles in new drug discovery, *Future Medicinal Chemistry*, 4(11) (2012) 1409-1438.

[60] Knudsen L.B., Lau J., The discovery and development of liraglutide and semaglutide, *Frontiers in Endocrinology*, 10 (2019) 155.

[61] Chatterjee J., Gilon C., Hoffman A., Kessler H., N-methylation of peptides: a new perspective in medicinal chemistry, *Accounts of Chemical Research*, 41(10) (2008) 1331-1342.

[62] Rautio J., Kumpulainen H., Heimbach T., Oliyai R., Oh D., Järvinen T., Savolainen J., Prodrugs: design and clinical applications, *Nature Reviews Drug Discovery*, 7(3) (2008) 255-270.

[63] Torchilin V.P., Recent advances with liposomes as pharmaceutical carriers, *Nature Reviews Drug Discovery*, 4(2) (2005) 145-160.

[64] Veronese F.M., Pasut G., PEGylation, successful approach to drug delivery, *Drug Discovery Today*, 10(21) (2005) 1451-1458.

[65] Craik D.J., Fairlie D.P., Liras S., Price D., The future of peptide-based drugs, *Chemical Biology & Drug Design*, 81(1) (2013) 136-147.

[66] Çelik S., Demirag A.D., Coşgun A.O., Özel A., Akyüz S., Computational investigation of the interaction mechanism of some anti-alzheimer drugs with the acetylcholinesterase enzyme, *Open Journal of Nano*, 8(1) (2023) 11-21.